Automated Quantitative Analysis of Single and Double Label Autoradiographs[1]

A. RÜTER, H. M. AUS, H. HARMS, M. HAUCKE, V. ter MEULEN, B. MAURER-SCHULTZE, H. KORR and A. KELLERER

SFB 105 Biomedical Image Processing Research Laboratory at the Institute of Virology and Immunobiology (A.R., H.M.A., H.H., M.H., V.T.M.), University of Würzburg Versbacher Landstrasse 7, and Institut für Medizinische Strahlenkunde der Universität Würzburg (B.M.-S., H.K., A.K.), Versbacher Landstrasse 5, 8700 Würzburg, West Germany

A method for the analysis of silver grain content in both single and double label autoradiographs is presented. The total grain area is calculated by counting the number of pixels at which the recorded light intensity in transmission dark field illumination exceeds a selected threshold. The calibration tests included autoradiographs with low (^{3}H-thymidin) and high (^{3}H-desoxyuridin) silver grain density. The results are proportional to the customary visual grain count. For the range of visibly countable grain densities in single labeled specimens, the correlation coefficient between the computed values and the visual grain counts is better than 0.96. In the first emulsion of the two emulsion layer autoradiographs of double labeled specimens (^{3}H-^{14}C-thymidin) the correlation coefficient is 0.919 and 0.906. The method provides a statistical correction for the background grains not due to the isotope. The possibility to record ^{14}C tracks by shifting the focus through the second emulsion of the double labeled specimens is also demonstrated. The reported technique is essentially independent of size, shape and density of the grains.

The visual evaluation of autoradiographs in the light microscope is a common and important technique in both experimental and clinical cytology. The grains observed in the photographic emulsions covering the biologic specimen reveal the location and amount of the incorporated radioactive label. Both single labeled and double labeled specimens can be used. In the former, only one isotope (^{3}H) and one thin emulsion layer are used. In the latter, two isotopes (^{3}H, ^{14}C) with different β-energies and two separate emulsion layers are used. The first thin layer covers the cells directly and serves to register the low energy ^{3}H electrons. The second, thick emulsion permits the registration of the high energy ^{14}C electrons. To prevent ^{3}H electrons from entering the second emulsion, the two emulsions are separated from each other by a neutral layer of gelatin. The size, shape, number and location of the visibly countable grains varies to a certain extent with the preparation technique, the exposure time, the film developer and the type of photographic emulsion. In visual, nonautomated evaluation of the autoradiographs, the investigator counts the visible clusters of silver filament. Especially at high grain densities, the dissection of these clusters into individual grains of similar size and shape is frequently impossible. The evaluation of all autoradiographs is further complicated by the presence of background grains in the emulsion that are not due to the charged particle flux from the isotope label. Therefore, an integrated silver grain area count, statistically corrected to minimize the effect of the background grain distribution, may be more closely correlated to the charged particle flux than the customary visual count (9). Using routine autoradiographs, the results presented in

this paper demonstrate the feasibility and advantage of applying computer aided techniques over the entire range of silver grain densities commonly assessed by visual counting.

MATERIAL AND METHODS

Autoradiography

Autoradiographs prepared from cells labeled with ^{3}H-thymidine (^{3}H-TdR) or ^{3}H-desoxyuridine (^{3}H-UdR) only and from cells double labeled with ^{3}H- and ^{14}C-thymidine (^{14}C-TdR) were used as the data sets for this study.

Single ^{3}H-labeled cells with a low grain density: Squashes were prepared from single isolated jejunal crypts of a NMRI mouse (27 g) that had received intraperitoneally 0.01 μCi ^{3}H-TdR (thymidine-methyl ^{3}H, specific activity 6.7 Ci/mmole) per gram body weight 1 hr before it was killed. Slides with Feulgen stained squashed crypts were dipped into diluted Ilford K2 emulsion (1:1 with water). After 96 days of exposure the autoradiographs were developed in amidol. Thirty specimens each from four low grain density preparations were scanned and analyzed.

Single ^{3}H-labeled cells with a high grain density: L 1210 ascites tumor cells from a B6D2F1 mouse (22 g) that had received intraperitoneally 5 μCi ^{3}H-UdR (^{3}H-6-desoxyuridine, specific activity 25.9 Ci/mmole) per gram body weight 30 min before it was killed were smeared on slides and autoradiographs were prepared as described above. The autoradiographs were exposed for 7 days and stained with Giemsa through the emulsion. A total of 75 specimens was scanned and counted from three different high density preparations.

Cells double labeled with ^{3}H- and ^{14}C-TdR: Jejunal crypt squashes from a NMRI mouse (22 g) that had received 4.5 μCi ^{3}H-TdR per gram body weight 4 hr and 0.15 μCi ^{14}C-TdR (thymidine-2-^{14}C, specific activity 51.3 mCi/mmole) per gram body weight 3 hr before it was killed were used for the two emulsion layer technique. Before applying the first thin (1.0–2.0 μm) emulsion layer the Feulgen stained squashes were processed as described above. After an exposure time of 3 days, the autoradiographs were developed and subse-

quently covered with a 5-μm thick gelatin layer and a second, thick layer of Ilford K2 emulsion (about 30-μm thick when dry and 15-μm after development). After 14 days of exposure the autoradiographs were developed and covered with a cover slip (see refs. 10, 14 for technical details).

The grains in the first, thin emulsion layer represent the ^{3}H-label and the tracks in the second, thick emulsion layer the ^{14}C-label. Thirty specimens from the first emulsion of two double label preparations were scanned and counted. The second emulsion of 10 specimens was also scanned and analyzed.

Cytophotometric Measurements

The autoradiographs were observed, visually evaluated and digitized in an Axiomat microscope (Firma C. Zeiss, Oberkochen, West Germany) interfaced to a PDP 11/50 (Digital, Maynard, Mass.). The autoradiographs were examined in both bright field (Halogen lamp) and dark field (Xenon lamp) transmission illumination. Each scene was digitized with a "Computer Eye" TV camera (Spatial Data, Goleta, Calif.) complete with a PDP 11 controller, TV monitor and shading correction hardware. The maximum raster size of the TV scan is 512 × 480 picture points (pixels) with a resolution of 256 gray levels. The spot size of the TV camera's electronic beam is 20 μm. The autoradiographs were scanned with a 50 × oil objective lens followed by a 3.2 × optovar lens. Therefore, approximately eight pixels are measured per micrometer in the specimen plane (spot size = 0.125 μm). This small spot size minimizes the aliasing problem associated with discrete sampling of the continuous microscope image (4, 8). Depending upon specimen size, the scanned field size varied between 180 × 180 and 512 × 480 pixels.

Cytophotometric Analysis

The digitized autoradiograph images were analyzed on the PDP 11/50 operating under RSX 11 M modified to include the TV camera as a peripherical device. The monitor images and the computer histograms and playback images were photographed with a CU5 Land camera (Polaroid, Cambridge, Mass.). All application software is written in Fortran IV.

RESULTS

In the bright field transmission microscope, grains appear as dark spots above the labeled cell nucleus. One field of a ^{3}H-labeled sample containing four nuclei is depicted in Figure 1A: nucleus K is unlabeled, N is weakly labeled, and both L and M are strongly labeled. The grains are randomly distributed throughout the relatively thin photographic emulsion. This emulsion is, however, thicker than the shallow depth of focus of the microscope lens used to view the autoradiographs. Consequently, some of the grains located either above or below the focal plane appear to be lighter than those grains located in the focal plane. These apparent differences in gray values made successful application of the customary cytophotometric methods (7, 16) for counting the grains impossible.

Compared to bright field illumination, in the dark field microscope the grains appear as brightly lighted, easy to recognize particles, and up to 20% more grains are visible at a single focus setting (Figs. 1B, 2A and 3). The underlying
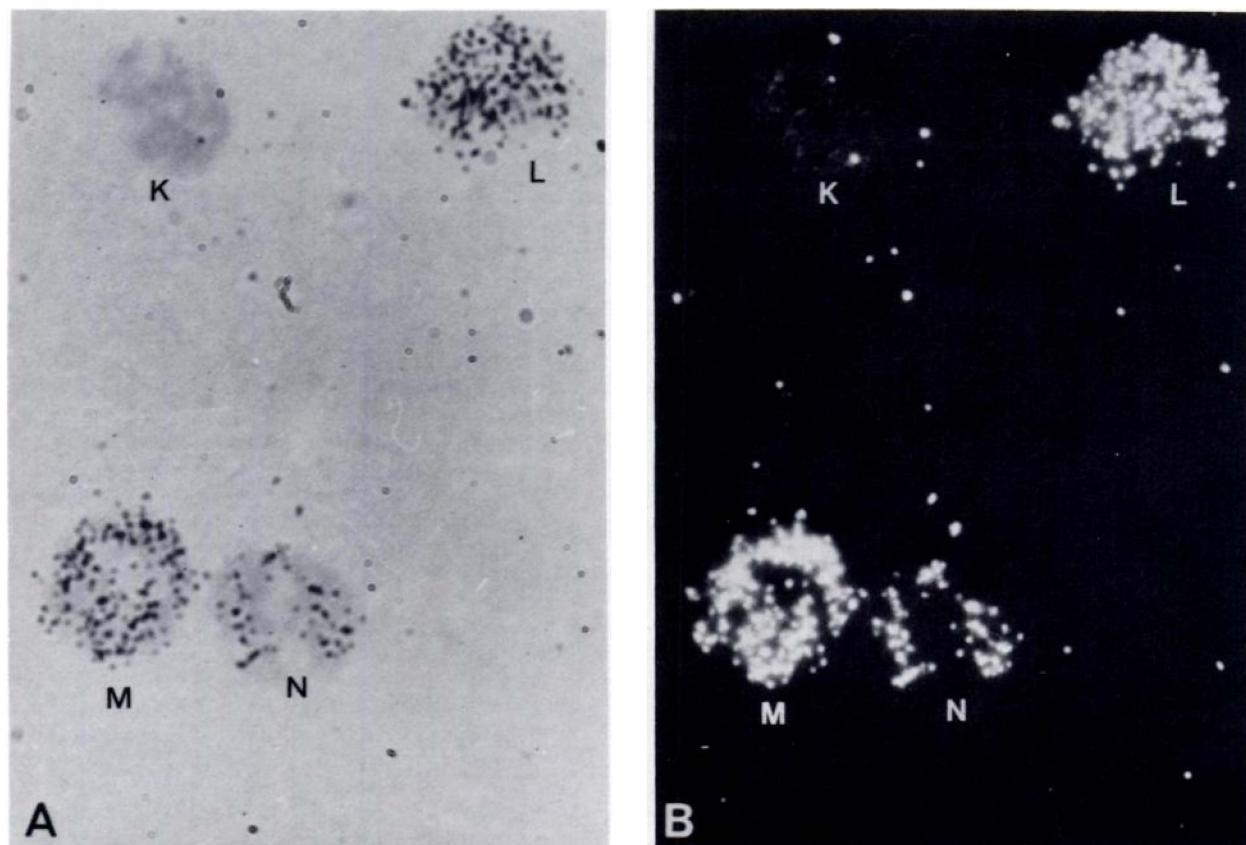

FIG. 1. Autoradiograph of single ^{3}H-label cell nuclei from the small intestine of a mouse as photographed in the transmission bright field (A) and dark field (B) microscope. Nucleus K is unlabeled, N is weakly labeled and both L and M are strongly labeled. Original magnification: × 250. Note: the additional grains that are visible in B but not in A and the halos of stray scattered light appearing between the grains in B.
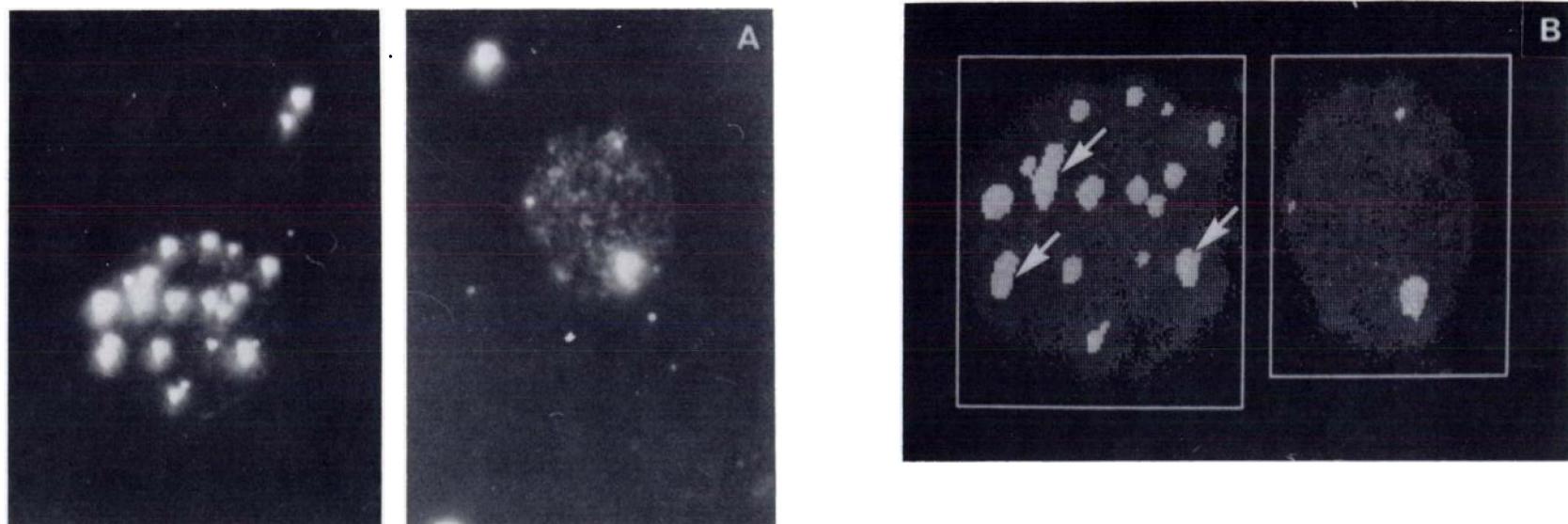
FIG. 2. A, two single ³H-label cells with low grain density; B, computer playback images of the scanned grain clusters and specimen areas in (A). The number of grains in a large cluster is estimated by dividing the number of pixels in a large cluster (arrows) by the mean grain size. The average size of the smaller areas containing only one grain is an estimate of the mean grain size.
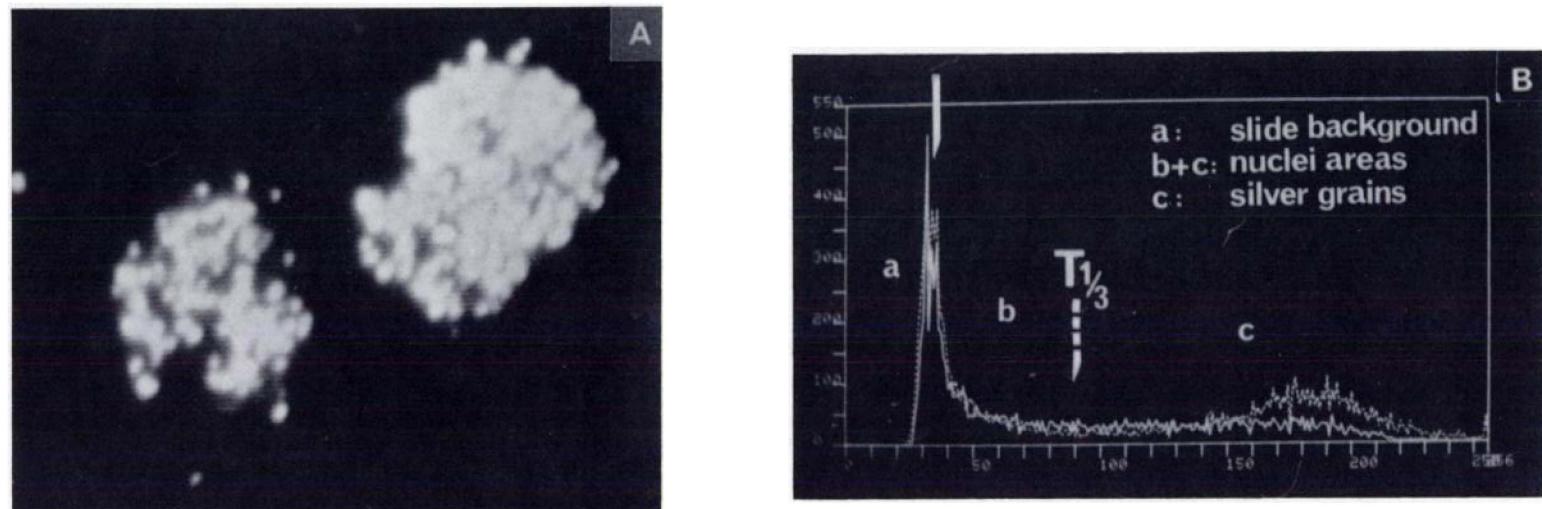

FIG. 3. A, single ³H-label cells with high grain density. B, histograms of the digitized images in A. The threshold $T_{1 \, 3}$ is determined by experiment as being sufficient to segment the silver grains from the specimen in the single labeled preparations. The solid line and the dotted line are from the left hand and right hand nuclei, respectively. The difference in the two histograms to the right of $T_{1 \, 3}$ is due to the different concentration of grains in the two specimens.

biologic specimen is, however, visually difficult to find and recognize. In addition, random reflections from the surface of the grains lead to scattered light halos around the grains which degrade the contrast-rich reflected light images. The closer the proximity of the grains to each other, the more these halos tend to overlap. This effect is especially noticeable in Figure 2A and can be minimized by the software methods described below. As in bright field microscopy, the dark field images can also be scanned, digitized and stored as arrays of gray values on a computer disk. A computer playback image of the nuclei in Figure 2A, scanned in the dark field microscope, is depicted in Figure 2B. The limited optical resolution of the available graphic terminal allows only background specimen and grains to be displayed. For the images shown in Figure 2B, two gray value thresholds were interactively selected to discriminate among the background, the specimen and the grains. The term background is used here to refer to

that part of the field which is covered neither by the cells nor by the grains from the labeled nuclei. Careful comparison of the grains in Figure 2A and B confirms that the images in Figure 2A have been correctly measured and that two thresholds have been found to segment correctly the relatively weakly labeled cells into grains, specimen and background despite the scattered light halos. In the remainder of this paper, the term "grain area" is defined to be the total number of all those pixels in the image which were detected as being brighter than the grain/specimen light intensity threshold. Note that the touching grains in Figure 2A appear as contiguous areas of detected pixels in the playback images (arrows in Fig. 2B). Each contiguous area, i.e., cluster, represents at least one grain. With the two selected thresholds, the computer program readily determines the total number of pixels in each cluster. The average number of pixels in the smaller areas is an estimate of the mean grain size. The number of
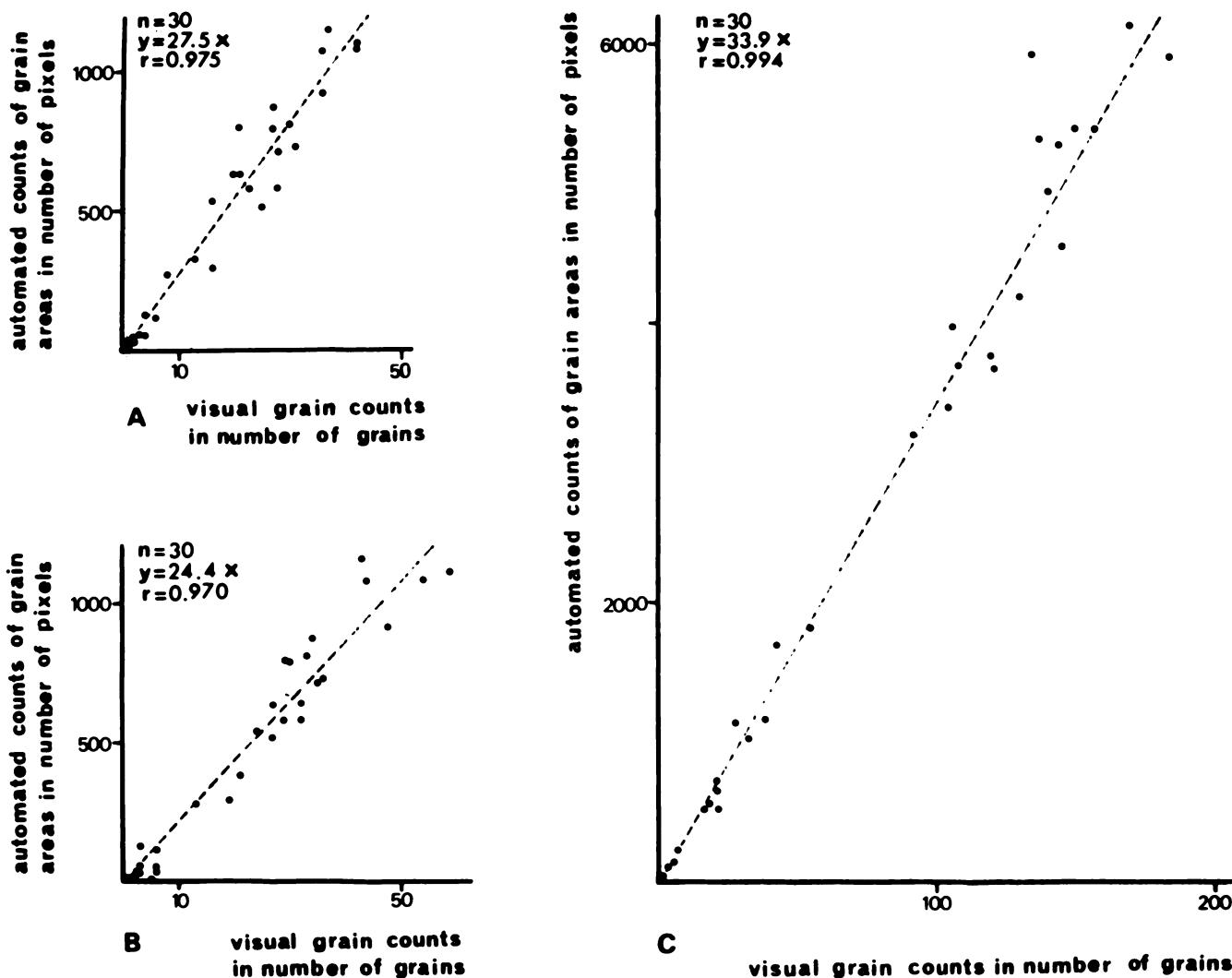

FIG. 4. Linear relationship of the pixel area *versus* visual grain counts in single label specimens. A and B are from ³H-thymidin labeled nuclei of the mouse small intestine as scanned in dark field, and visually counted in the bright field and dark field microscope, respectively. C, is from ³H-desoxiuridin labeled mouse leukemia cells scanned in dark field and visually counted in bright field. n is the sample size, r is the correlation coefficient between the visual counts and the computed grain areas, y = mx is the equation describing the dashed line.

grains contained in a large cluster (arrows Fig. 2B) can be estimated by dividing the number of pixels in the large cluster by the mean grain size. This method works well for small and intermediate grain densities. Compared to counting the number of grains, however, the total grain area, as explained below, is more generally applicable.

Typical dark field images for the highest visibly countable grain density are shown in the strongly labeled specimen of Figure 3A. In this autoradiograph the grains are closer together and the effect of scattered light is less than in the weakly labeled samples. Segmentation of the specimen and grains is achieved using the T_{13} threshold shown in Figure 3B. The histogram is calculated by determining the frequency of occurrence of the measured gray values in the scanned cell image. In this study, the possible gray values range from 0

(darkest) to 255 (brightest). The different grain concentrations of the two clusters of Figure 3A results in the difference of the two histograms to the right of c in Figure 3B.

For the single label specimens, the scattered reflected light is adequately eliminated by using a specimen/grain threshold of 33% of the measured optical density range (T_{13} in Fig. 3B). This absolute threshold varies slightly because of fluctuation in the plasma lamp intensity and the sensitivity of the TV camera. The linear relationship between the grain area and the visual grain count is shown in Figure 4. Relative to the visual count in both bright field (Fig. 4A) and dark field (Fig. 4B), the correlation coefficient, r, of the automated grain area counts in the autoradiographs with low grain density is 0.975 and 0.97, respectively. Similarly, the correlation coefficient is 0.994, over the range of possible visual counts in the autora-
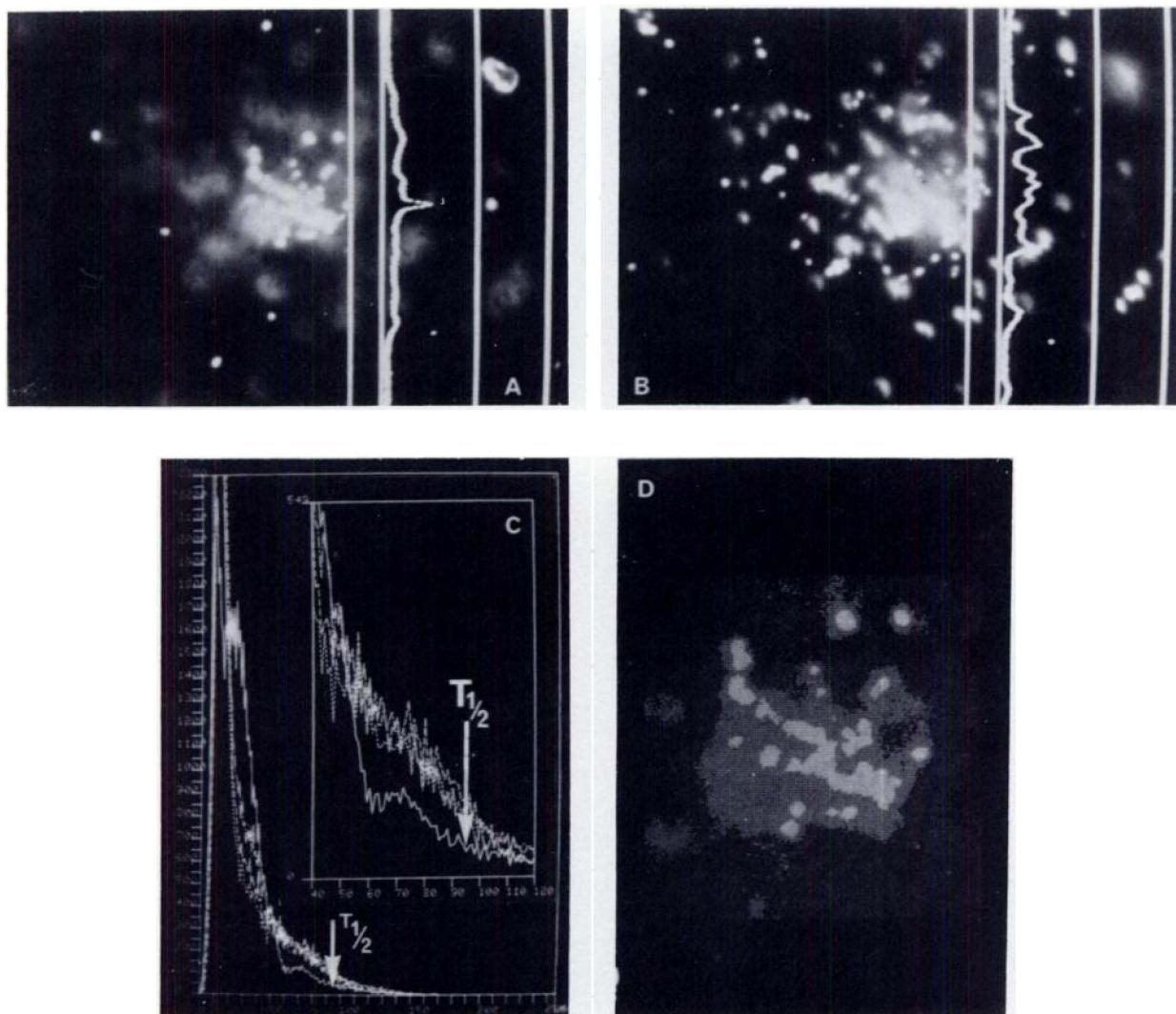

FIG. 5. A, section of the first emulsion from a mouse jejunum nucleus double labeled with ^{3}H- and ^{14}C-TdR photographed from the screen of the TV monitor. B, photograph of the section located approximately in the middle of the second, thick emulsion and above the same labeled nucleus as in A. The vertical lines in A and B are, from left to right: TV scan line, minimum intensity (dark), measured optical intensity at the TV scan line, maximum digitized intensity and maximum possible intensity. C, histograms of the digitized optical intensities from the first emulsion (solid line) and from three focus settings in the second emulsion. The inset shows the detail in the optical intensity range 40 to 120. The threshold T_{12} refers to the lower curve from the first emulsion only and is determined by experiment to be sufficient for segmenting the silver grains from the specimen in the double label preparations. D, playback of grains in A using the T_{12} threshold.

diograph with high grain density (Fig. 4C). The experiment has been repeated on three additional low density and two additional high density preparations. In all cases the correlation coefficient is greater than 0.96.

The situation is considerably more complicated in two emulsion layer autoradiographs of double labeled specimens. Digitized scans from the first emulsion (Fig. 5A) contain unwanted scattered light from the grains in the second emulsion (Fig. 5B), which produces the local peak in the corresponding histogram (solid line between 60 and 98 in Figure 5C, inset). This extra peak does not occur in the histogram from the single labeled specimen (Fig. 3B). A specimen/grain threshold of approximately 50% (T_{12} in Fig. 5D) of the maximum measured optical intensity is found to be required to eliminate the scattered light originating in the second emulsion from the scanned grain image of the first emulsion. The

resulting correlation coefficient between visual counts and computer grain area is $r = 0.919$ in the first emulsion of the double labeled specimen. In the second test preparation, $r = 0.906$. Finding and identifying the specimen is extremely difficult in the dark field illumination.

Being distributed throughout the second, approximately 15-μm thick emulsion, all the grains from the ^{14}C β-tracks are never simultaneously in focus (Fig. 5B). At a single focus setting, the scattered light from the grains not in the focal plane makes it impossible to find thresholds that adequately discriminate among the focussed, unfocussed and background grains (Fig. 5C, inset). In the autoradiographs of the specimen labeled with ^3H and ^{14}C-TdR, 10 focus settings are required to cover the entire depth of the second emulsion. The digitized images from these 10 focus settings are used to calculate one composite computer image of all the grains in the second
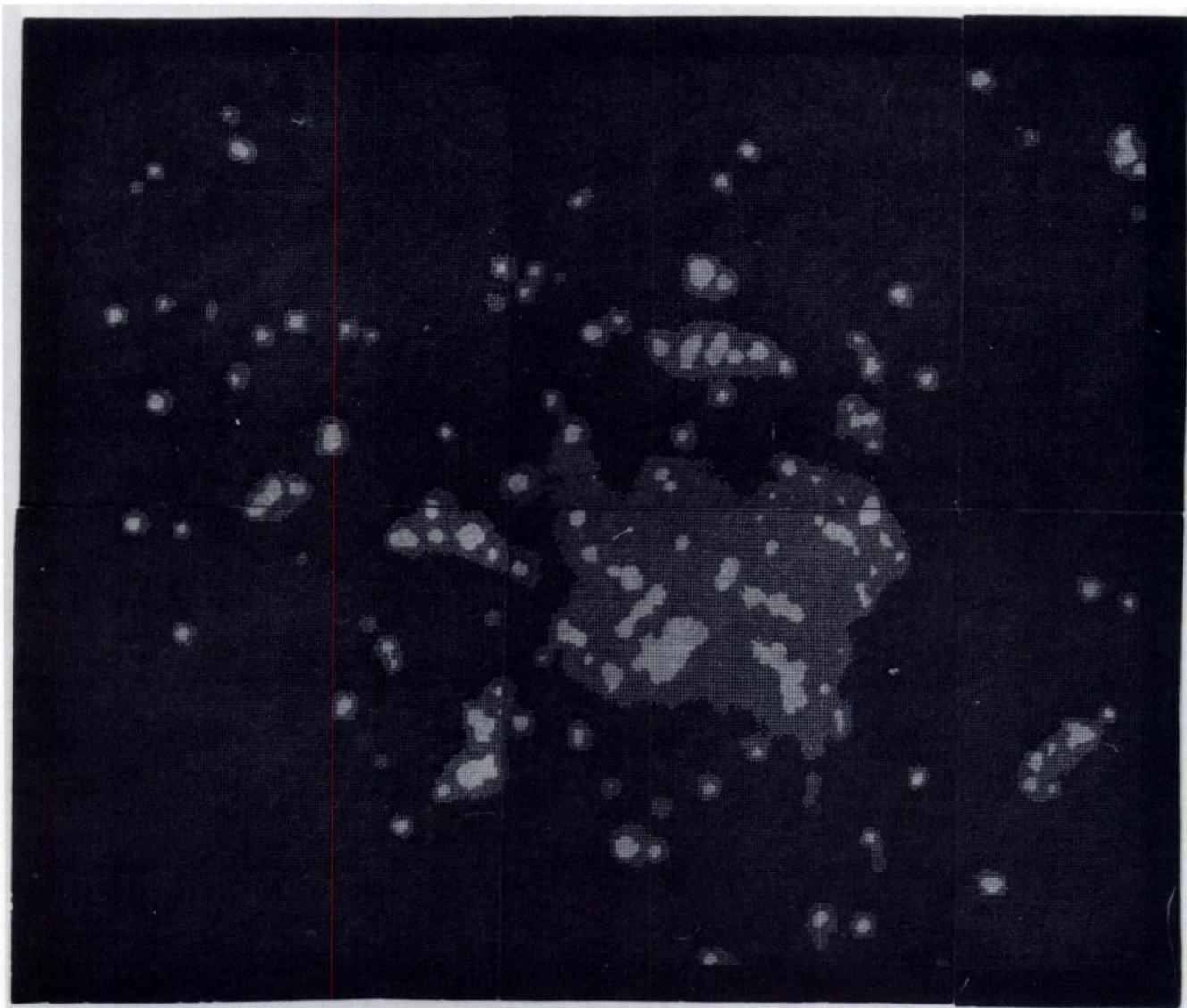

FIG. 6. Computer calculated composite image of the 10 scans from the second emulsion of the double label specimen in Figure 5. The computer selects the maximum intensity from the 10 scans at each pixel in the scanned field to produce this single image. The 10 scans are sufficient to record all the grains in the second emulsion above the labeled specimen. This figure is a collage of six photographs from adjacent sections in the resulting computer image displayed on the graphic terminal screen.

emulsion. The computer algorithm searches through all ten scans for the maximum optical intensity at each pixel and stores these maxima as a new array of gray values. Tracks of silver grains are clearly evident in the graphic terminal display of this composite array (Fig. 6). Visual comparison of the microscope and playback image confirms that all the grains in the second and none of the grains in the first emulsion have been measured and retained. Similar results were obtained for the 10 scanned double label specimens. Further reduction of the images to include only the X, Y and Z coordinates of each grain is also currently provided.

The restriction of limiting the scanned field to contain only one labeled specimen was necessary in order to simplify the initial test and calibration data sets. As demonstrated in Figure 7, the same measurement and software methods also apply to the microscope fields that are scanned sequentially without reference to cell position. As seen in the computer printout, the software calculates the positions and approximate sizes of the specimens, as well as the total grain area above each labeled specimen. The remaining areas in the scans, which nevertheless contain silver grains not due to the isotope label, are used to calculate the background density. The frequency of background grains is the area of these detected grains relative to the size of the area not containing any cells (Fig. 7). This permits a statistical correction of the

computed grain areas by subtracting the background from the recorded grain areas above the labeled specimens. This statistical background correction is recalculated for each scan.

DISCUSSION

The results of this study demonstrate the usefulness of computer aided cytophotometric techniques in the evaluation of autoradiographs of both single and double labeled specimen with ^{3}H and ^{14}C TdR. Taking advantage of the enhanced contrast and resolution in the dark field microscope, the method accurately localizes the grains in both emulsions and determines the total grain area in the first emulsion. Statistical correction for the background grains not due to the isotope label can also be provided. Using 3-dimensional software algorithms, the preliminary data demonstrate the potential of recording ^{14}C tracks in the second emulsion. Results from the track-counting algorithms currently being developed indicate that the computer can (a) count the number of tracks in the 3-dimensional space above the double label specimen, (b) count the number of grains in the tracks and (c) determine the length and direction of the tracks. The technique is essentially independent of the grain's size, shape and density. The results reported here were obtained using digitized images of routine autoradiographs as test data sets.

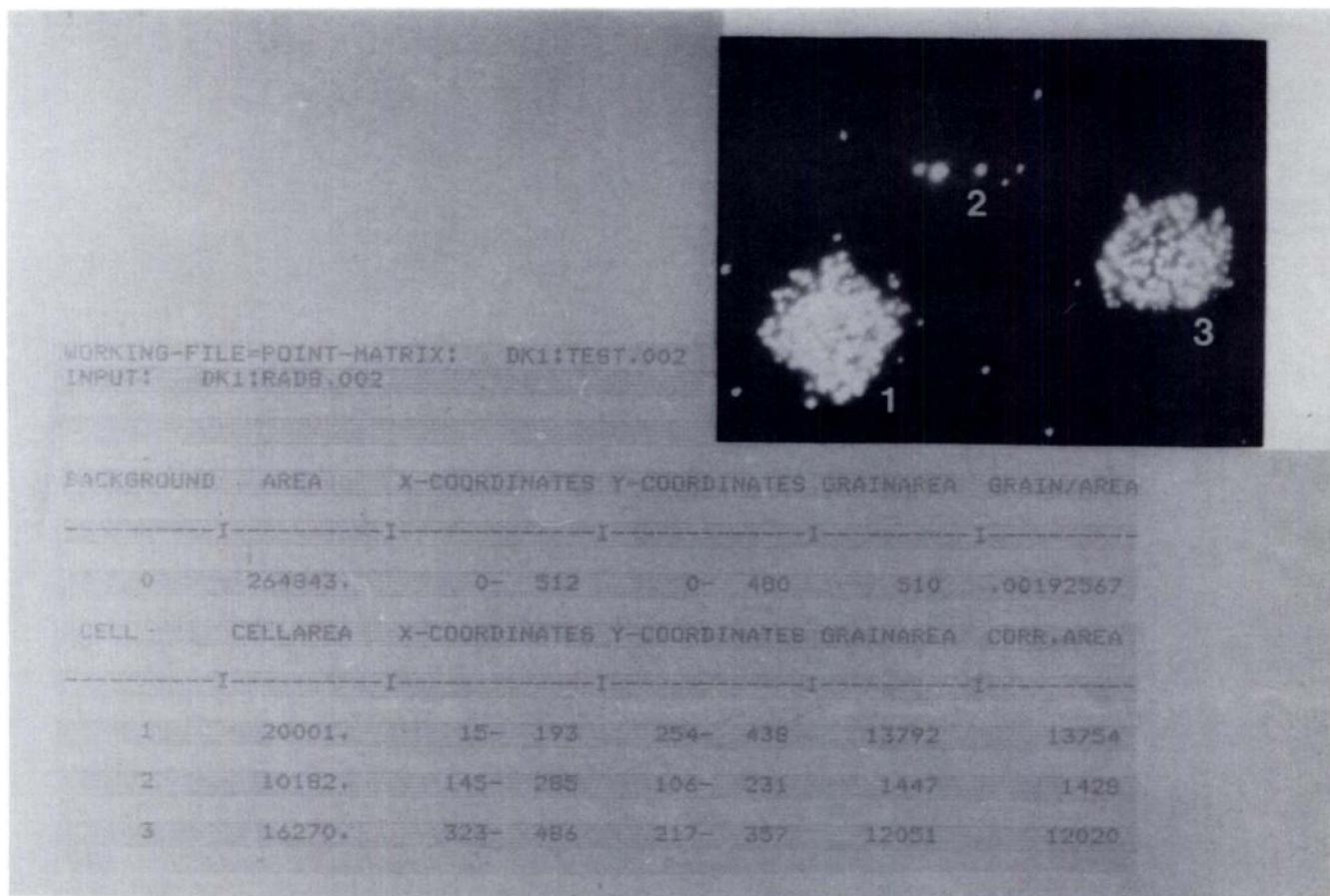Because of the increased depth of focus in dark field illu-

FIG. 7. Printout from the automated count of the three labeled cells shown in the TV monitor inset photograph. Original magnification: × 160. Corrected area (Corr. area) is the detected grain area minus the neighborhood background count.

mination, the described computer analysis requires only one scan of the thin emulsion used to detect the ^{3}H grains. The total grain area, calculated as the number of pixels at which the measured gray value exceeds the properly selected light intensity threshold, provides an accurate measure of the incorporated labeled component. Using the total area has the advantage of not requiring the identification of the individual grains. The separation of clusters of grains into individual grains at high concentrations is frequently not possible. The reported results correlate closely with the visual grain counts. The error introduced by the background grains (12), a non-specific phenomenon, can be statistically minimized by subtracting the calculated background grain densities from the computed grain areas above the labeled specimen. Locating the specimen and identifying the colors in the stained cells is essential if a meaningful correlation between the isotope label and the different specimens is to be realized on a routine basis.

The accuracy of the described method is contingent upon the proper selection of the specimen/grain thresholds that minimize the effects of the scattered light halos around the grains. These halos appear in dark field illumination as a result of the random reflection of the incident light from the rough surfaces of the grains. Rather than smooth solid particles, the grains are actually random curls of silver filaments with uneven reflective surfaces. More sophisticated specimen/grain thresholds than the empirical one reported here have also been investigated (11), but none leads to a significant improvement in the linear proportionality and correlation between the computer and visual counts. The automatically selected thresholds are unsatisfactory because variations in the stain uptake produce too many extraneous peaks immediately to the right of the large background peak in the histogram (Fig. 3B). The thresholds used in this investigation were selected empirically.

Attempts to count grains in single labeled autoradiographs have been reported by several groups (1–3, 5, 6, 9, 15). Of these, only Dörmer and Thiel (3) have attempted measurements in transmission dark field illumination. In their work, the light reflected from the grains is measured with an aperture spot size equal to the size of the labeled specimen. This single integrated light intensity measurement has the advantage of simplicity; however, it has the drawback of including light intensity from the grains, as well as from the specimen and the halos in each measurement. Similarly, none of the methods reported by Lipkin *et al.* (5), Prensky (6), Bisignani and Greenhouse (1), Stengel-Rutkowsky *et al.* (15) and Rogers (9) distinguishes satisfactorily among specimens, grains and optical artifacts. The realization that these problems can only be minimized by the application of software techniques led, in fact, to the present investigation.

LITERATURE CITED

1. Bisignani WT, Greenhouse SC: The hybrid resolution approach to automated autoradiographic analysis. J Histochem Cytochem 24:152, 1976
2. Dörmer P: Photometric methods in quantitative autoradiography, microautoradiography and electron probe analysis, Their Application to plant Physiology. Edited by U Lüttge. Springer Verlag, Berlin, 1972, p 7–48
3. Dörmer P, Thiel E: Methods of quantitative autoradiography using incident light microphotometry. J Histochem Cytochem 24: 145, 1976
4. Korn GA: Random-Process Simulation and Measurements. McGraw-Hill, New York, 1966, p 151
5. Lipkin LE, Lemkin P, Carman G: Automated autoradiographic grain counting in human determined context. J Histochem Cytochem 22:755, 1974
6. Prensky W: Automated image analysis in autoradiography. Exp Cell Res 68:388, 1971
7. Preston K: Digital picture analysis in cytology, Topics in Applied Physics. Digital Picture Analysis (vol 11). Edited by A Rosenfeld. Springer Verlag, Berlin, 1976, p 209
8. Rabiner LR, Gold B: Theory and Application of Digital Signal Processing. Prentice-Hall, London, 1975, p 26
9. Rogers WA: A simple photometric device for the quantitation of silver grains in autoradiographs of tissue sections. Exp Cell Res 24:288, 1961
10. Rogers AW: Techniques of Autoradiography (2nd ed). Elsevier, Amsterdam, 1973
11. Rosenfeld A, Kak AC: Digital Picture Processing. Academic Press, New York, 1976, p 258
12. Ruthmann A: Methods in Cell Research. G Bell and Sons Ltd, London, 1970, p 209
13. Schultze B: Autoradiography at the Cellular Level in Physical Techniques in Biological Research. Edited by AW Pollister. Academic Press, New York, 1969, vol III
14. Schultze B, Maurer W, Hagenbusch H: A two emulsion autoradiographic technique and the discrimination of the three different types of labeling after double labeling with ^{3}H- and ^{14}C-thymidine. Cell Tiss Kinet 9:245, 1976
15. Stengel-Rutkowski S, Gundlach H, Zang KD: Quantitative electronic analysis of chromosome autoradiographs using a television image analysis computer. Exp Cell Res 87:313, 1974
16. Thiessen G, Thiessen H: Microspectrophotometric cell analysis, Progress in Histochemistry and Cytochemistry. G Fischer, Stuttgart, 1977, p 37